Rapid Communication

Determination of the load-independent hardness by analyzing the nanoindentation loading curves: A case study on fused silica

Yunbiao DUAN[a], Danyu JIANG[b,*], Jin HU[a]

[a]*Faculty of Materials Science and Engineering, Kunming University of Science and Technology, Kunming 650093, China*
[b]*State Key Laboratory of High Performance Ceramics and Superfine Microstructure, Shanghai Institute of Ceramics, Shanghai 200050, China*

Abstract: The nanoindentation loading curves measured on fused silica were analyzed based on the theoretical relationship derived by Malzbender *et al.* (*J Mater Res* 2000, **15**: 1209–1212). It was found that the ratio of the applied load to the square of the displacement, $P/(h + h_d)^2$, does not keep constant during loading segment of the nanoindentation test. Considering the existence of the indentation size effect, an empirical method for the determination of the load-independent hardness by analyzing the nanoindentation loading curves was proposed.

Keywords: nanoindentation; loading curve; indentation size effect (ISE); fused silica

1 Introduction

It has been generally suggested that the loading portion of the load–displacement curve obtained during nano-indentation test, with ideally sharp conical indenter (e.g., the Berkovich indenter), can be well described by [1–4]:

$$P = \alpha h^2 \qquad (1)$$

where P is the indentation load, h is the indenter displacement, and the proportionality constant α depends on the material tested as well as the type of indenter. By writing the total indentation depth h as the sum of the contact depth h_c and the displacement of the surface at the perimeter of the contact h_s (Fig. 1(a)), Malzbender *et al.* [5] derived an explicit expression for the constant α:

$$\alpha = E_r \left(\frac{1\pi}{\sqrt{24.5}} \sqrt{\frac{E_r}{H}} + \varepsilon \sqrt[4]{\frac{H}{E_r}} \right)^{-2} \qquad (2)$$

where ε is an indenter geometrical constant which takes a value of 0.75 for the Berkovich indenter [6], E_r is the reduced Young's modulus given by

$$\frac{1}{E_r} = \frac{1-\nu^2}{E} + \frac{1-\nu_I^2}{E_I} \qquad (3)$$

where E and ν are Young's modulus and Poisson's ratio, respectively, of the indented specimen, and $E_I = 1171$ GPa and $\nu_I = 0.07$ are those of the diamond indenter [6]. H is the hardness defined as

$$H = \frac{P}{A_c} = \frac{P}{24.5 h_c^2} \qquad (4)$$

In order to take into account the fact that a real indenter is never perfect due to some tip rounding (Fig.

* Corresponding author.
E-mail: dyjiang@mail.sic.ac.cn

1(b)), Malzbender *et al.* [5] further suggested that the term h^2 in Eq. (1) should be replaced with $(h + h_\mathrm{d})^2$, where h_d is called the effective truncation length of the indenter tip and its physical meaning is explained in Fig. 1(b). Thus, the load–displacement relation can be finally described as

$$P = E_\mathrm{r} \left(\frac{1\pi}{\sqrt{24.5}} \sqrt{\frac{E_\mathrm{r}}{H}} + \varepsilon \sqrt{\frac{\pi}{4}} \sqrt[4]{\frac{H}{E_\mathrm{r}}} \right)^{-2} (h + h_\mathrm{d})^2 \qquad (5)$$

Equation (5) predicts that $P/(h + h_\mathrm{d})^2$ should be a constant during the loading segment of a nanoindentation test. However, such a prediction has been verified only based on finite element simulation [5,7] and, up to now, little experimental verification has been conducted. Further, as mentioned by Malzbender *et al.* themselves [5], one of the most important assumptions in deriving Eq. (5) is that the hardness can be treated to be a constant, independent of indentation depth, despite the fact that *indentation size effect* (ISE) in the measured hardness is known to occur. Thus, in this communication, the nanoindentation data obtained on fused silica were analyzed to examine the applicability of Eq. (5) in describing the nanoindentation loading curves. By taking the indentation size effect into account, an empirical method for determining the load-independent hardness based on Eq. (5) was proposed.

2 Experimental

A commercial fused silica slide was used as the test sample. Fused silica is a reference material widely adopted in experimental verifications of nanoindentation theories [6,8–10]. Considering Young's modulus and Poisson's ratio might be generally expected to remain constants with scale, the literature reported data for fused silica, $E = 72$ GP and $\nu = 0.17$ were adopted for the present study.

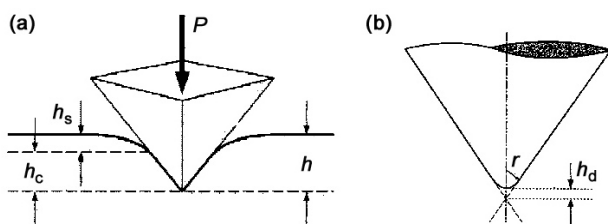Nanoindentation tests on fused silica were carried out using a Berkovich diamond tip with a commercial nanoindenter (Nano Indenter G200, Aglient, Santa Clara, CA, USA). For each test, the indenter was linearly loaded to the prescribed maximum value, ranging from 50 to 400 mN, within 10 s, held at the maximum load for 10 s, and then unloaded linearly within 10 s.

Figure 2 shows a typical load–displacement curve measured with a maximum load of 100 mN.

3 Results and discussion

Using Eq. (5) to describe the experimentally measured loading curves needs to know the value of the effective truncation length h_d, which can be estimated using the following relation [11–14]:

$$S = \beta (h_\mathrm{c} + h_\mathrm{d}) \qquad (6)$$

where S is the contact stiffness and β is a constant dependent on the reduced Young's modulus. Equation (6) predicts a linear relationship between S and h_c and h_d can be estimated easily from the intercept.

The unloading portion of each measured load–displacement curve was analyzed according to the traditional Oliver–Pharr method [6] to yield the contact stiffness S and the contact depth h_c corresponding to each prescribed maximum load and the results are shown in Fig. 3. As can be seen, a good linear relationship exists between these two parameters, being in good agreement with Eq. (6). Then h_d was calculated to be 22.09 nm from the best-fit results with Eq. (6).

Using $h_\mathrm{d} = 22.09$ nm, the $P/(h + h_\mathrm{d})^2$ value for each experimental datum in the loading portion of each measured load–displacement curve was calculated and the results are shown in Fig. 4. Clearly, the resultant
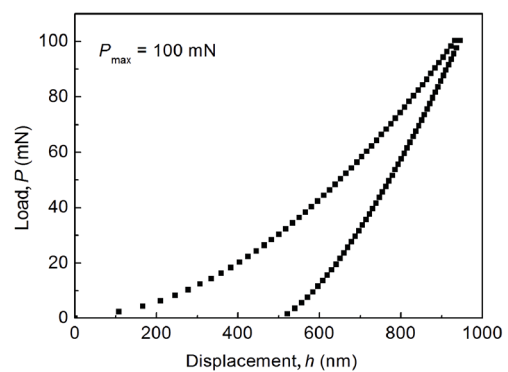

Fig. 1 Schematic diagrams showing (a) $h = h_\mathrm{c} + h_\mathrm{s}$ and (b) the geometry of a rounded indenter tip.

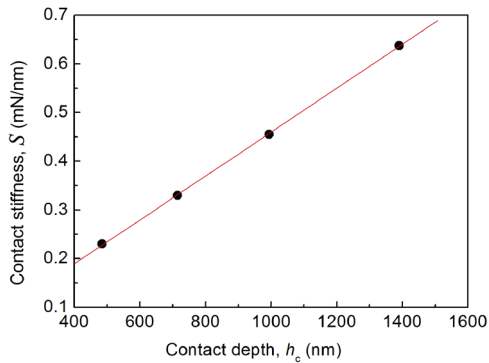**Fig. 2** Typical load–displacement curve measured for fused silica ($P_\mathrm{max} = 100$ mN).

Fig. 3 Relationship between the contact stiffness S and the contact depth h_c. The solid line is obtained by regression analysis of the experimental data.
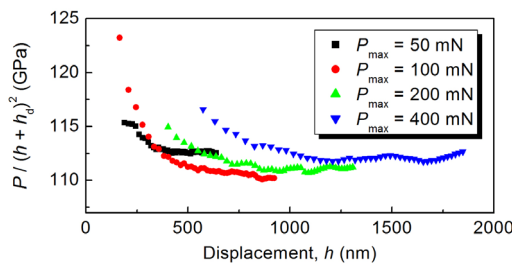

Fig. 4 Experimentally determined $P/(h+h_d)^2$ as functions of displacement h for different maximum load ($h_d = 22.09$ nm).

$P/(h + h_d)^2$ exhibits a decreasing tendency with h, especially within the small displacement (low load) region.

Noting that, in Eq. (5), $\varepsilon = 0.75$ is a constant dependent only on the indenter geometry and, as mentioned above, Young's modulus might be generally expected to remain constant with scale, thus the decreasing tendency in $P/(h + h_d)^2$ shown in Fig. 4 seems to imply that, if Eq. (5) is really suitable for describing the nanoindentation loading curve, the hardness H included in Eq. (5) cannot be treated as a constant. In fact, the load dependence of the measured hardness has been frequently observed for different materials [15,16]. There is reason to believe that such a load dependence may also exist during the loading segment of a nanoindentation test.

In order to confirm this idea, the hardness H was calculated as functions of indentation load P based on Eq. (5) using the values of $P/(h + h_d)^2$ given in Fig. 4. The results are shown in Fig. 5. Clearly, the calculated hardness exhibits a significant load dependence.

The load dependency of the measured hardness, i.e., ISE, has been widely studied and some phenomenological explanations for the origin of the ISE have been proposed [15–18]. It has been found that a second-order
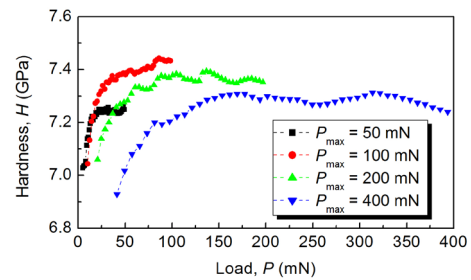

Fig. 5 Load dependency of the hardness calculated based on Eq. (5) using measured $P/(h+h_d)^2$.

polynomial is sufficiently suitable for describing the relationship between the test load P and the contact depth h_c [16,19,20]:

$$P = a_0 + a_1 h_c + a_2 h_c^2 \tag{7}$$

where a_0, a_1, and a_2 are constants. Especially, the coefficient a_2 is considered to be related with the load-independent hardness H_T of the test material:

$$H_T = k a_2 \tag{8}$$

where k is a constant dependent on the indenter geometry. For Berkovich indenter, $k = 1/24.5$.

Using the values of the measured hardness H given in Fig. 5, the contact depth h_c corresponding to each datum point is calculated with Eq. (4) and the result is shown as a function of the load in Fig. 6. The solid line in this plot is obtained by a conventional polynomial regression according to Eq. (7). Clearly, Eq. (7) is proven sufficiently suitable for the representation of the data.

Using the best-fit value of a_2, $a_2 = 1.7447 \times 10^{-4}$ mN/nm^2, the true hardness of the fused silica can be determined from Eq. (8) to be 7.12 GPa, which is somewhat smaller compared with the reported values of the measured hardness, about 8.5 GPa [6,21]. This may be understood by noting that, in most cases [16,19,20], the load-independent hardness determined with Eqs. (7) and (8) is always smaller than the load-dependent hardness value calculated with Eq. (4).
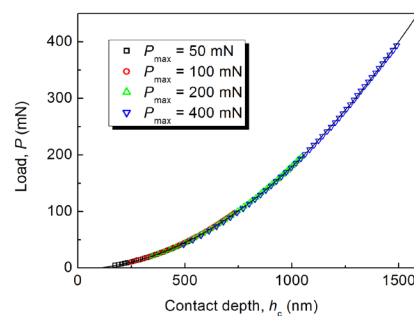

Fig. 6 Relationship between load P and contact depth h_c calculated with the experimental data given in Fig. 5.

4 Concluding remarks

Based on the above analyses, it may be concluded that:

(1) The hardness H included in Eq. (5) may not be treated as a constant. As a result, the measured $P/(h + h_d)^2$ exhibits a significant variation with displacement h.

(2) Equation (5) can be used to determine the load dependence of the hardness H and the relationship between the contact depth and the applied load during the loading segment of a nanoindentation test. The latter can then be used to determine the load-independent hardness of the test material.

It should be pointed out that the analyses conducted in the present study are still somewhat simple and, at least, further studies should be carried out to consider the effect of other parameters included in Eq. (5), the indenter geometry constant ε and the effective truncation length h_d, on the reliability of the load-independent hardness determination.

References

[1] Hainsworth SV, Chandler HW, Page TF. Analysis of nanoindentation load-displacement loading curves. *J Mater Res* 1996, **11**: 1987–1995.

[2] Zeng KY, Rowcliffe D. Analysis of penetration curves produced by sharp indentations on ceramic materials. *Philos Mag A* 1996, **74**: 1107–1116.

[3] Cheng YT, Cheng CM. Relationships between hardness, elastic modulus, and the work of indentation. *Appl Phys Lett* 1998, **73**: 614–616.

[4] Fischer-Cripps AC. Illustrative analysis of load-displacement curves in nanoindentation. *J Mater Res* 2007, **22**: 3075–3086.

[5] Malzbender J, de With G, den Toonder J. The $P–h^2$ relationship in indentation. *J Mater Res* 2000, **15**: 1209–1212.

[6] Oliver WC, Pharr GM. An improved technique for determining hardness and elastic modulus using load and displacement sensing indentation experiments. *J Mater Res* 1992, **7**: 1564–1583.

[7] Jha KK, Suksawang N, Agarwal A. Analytical method for the determination of indenter constants used in the analysis of nanoindentation loading curves. *Scripta Mater* 2010, **63**: 281–284.

[8] Gadelrab KR, Bonilla FA, Chiesa M. Densification modeling of fused silica under nanoindentation. *J Non-Cryst Solids* 2012, **358**: 392–398.

[9] Park JS, Lee YH, Kim Y, *et al*. Prediction of bluntness for pyramidal indenters from nanoindentation curves. *Surf Coat Technol* 2012, **211**: 148–151.

[10] Jia YF, Cui YY, Xuan FZ, *et al*. Comparison between single loading–unloading indentation and continuous stiffness indentation. *RSC Adv* 2017, **7**: 35655–35665.

[11] Bull SJ, Page TF, Yoffe EH. An explanation of the indentation size effect in ceramics. *Philos Mag Lett* 1989, **59**: 281–288.

[12] Herrmann K, Jennett NM, Wegener W, *et al*. Progress in determination of the area function of indenters used for nanoindentation. *Thin Solid Films* 2000, **377–378**: 394–400.

[13] Sawa T, Tanaka K. Simplified method for analyzing nanoindentation data and evaluating performance of nanoindentation instruments. *J Mater Res* 2001, **16**: 3084–3096.

[14] Gong JH, Miao HZ, Peng ZJ. On the contact area for nanoindentation tests with Berkovich indenter: Case study on soda-lime glass. *Mater Lett* 2004, **58**: 1349–1353.

[15] Gong JH, Wu JJ, Guan ZD. Examination of the indentation size effect in low-load Vickers hardness testing of ceramics. *J Eur Ceram Soc* 1999, **19**: 2625–2631.

[16] Peng ZJ, Gong JH, Miao HZ. On the description of indentation size effect in hardness testing for ceramics: Analysis of the nanoindentation data. *J Eur Ceram Soc* 2004, **24**: 2193–2201.

[17] Fröhlich F, Grau P, Grellmann W. Performance and analysis of recording microhardness tests. *Phys Stat Sol (a)* 1977, **42**: 79–89.

[18] Li H, Bradt RC. The microhardness indentation load/size effect in rutile and cassiterite single crystals. *J Mater Sci* 1993, **28**: 917–926.

[19] Jiang DY. Recent progresses in the phenomenological description for the indentation size effect in microhardness testing of brittle ceramics. *J Adv Ceram* 2012, **1**: 38–49.

[20] Shao LQ, Jiang DY, Gong JH. Nanoindentation characterization of the hardness of zirconia dental ceramics. *Adv Eng Mater* 2013, **15**: 704–707.

[21] Keryvin V, Charleux L, Hin R, *et al*. Mechanical behaviour of fully densified silica glass under Vickers indentation. *Acta Mater* 2017, **129**: 492–499.